JREE: Vol. 1, No. 1 (December 2014) 30-42

Research Article

Journal of Renewable Energy and Environment

Journal Homepage: www.jree.ir

Three Dimensional Computational Fluid Dynamics Analysis of a Proton Exchange Membrane Fuel Cell

Sajjad Rezazadeh[*a], Iraj Mirzaee[a], Nader Pourmahmoud[a], Nima Ahmadi[a]

[a]*Department of Mechanical Engineering, Urmia University, Urmia, Iran*

Article History

Received: 22 July 2013 Received in revised form: 2 Dec. 2013 Accepted: 16 April 2014 Available online: 21 June. 2014

A B S T R A C T

A full three-dimensional, single phase computational fluid dynamics model of a proton exchange membrane fuel cell (PEMFC) with both gas distribution flow channels and Membrane Electrode Assembly (MEA) has been developed. A single set of conservation equations which are valid for the flow channels, gas-diffusion electrodes, catalyst layers, and the membrane region are developed and numerically solved using a finite volume based computational fluid dynamics technique. In this research, some parameters such as oxygen consumption, water production, temperature distribution, ohmic losses, anode water activity, cathode over-potential and the fuel cell performance for straight single cell were investigated in more detail. The numerical simulations reveal that these important operating parameters are highly dependent on each other and the fuel cell efficiency is affected by kind of species distribution. So for, especial uses in desirable voltages, for preventing from the unwilling losses, these numerical results can be useful.

Finally the numerical results of proposed CFD model have been compared with the published experimental data that represent good agreement.

Keywords: PEM fuel cell, Ohmic loss, water activity, CFD, Fuel cell performance

1. Introduction

In past decades, the researchers have tried to find the new technology as the solution to the energy and environmental problems [1-4]. In this way, they could gain the fuel cell technology.

The different types of fuel cells are distinguished by the electrolytes used. Among them, the Proton Exchange Membrane Fuel Cell (PEMFC), which is the focus of this paper, is described by the use of a polymer electrolyte membrane [5-9].

As shown in figure 1, a typical PEM fuel cell is consisting of 9 regions: anode (bipolar plate, gas channel, gas diffusion layer, and catalyst layer), membrane, cathode (bipolar plate, gas channel, gas diffusion layer, and catalyst layer).

The humidified air and hydrogen (to keep the membrane water swollen in order to enhance sufficient proton conductivity) enter the cathode and anode channels, respectively. The hydrogen molecule diffuses through the anode diffusion layer towards the catalyst layer where it divides into H+ and electrons:

$$H_2 \rightarrow 2H^+ + 2e^- \quad (1)$$

Since the membrane is considered impermeable for reactant gases and electrons, only protons can migrate through the membrane. The produced electrons travel through the conductive diffusion layer and an external circuit.

The main electro chemical reaction occurs on the cathode catalyst layer. The oxygen diffuses through

[*] Corresponding author. *Email: sor.mems@gmail.com*

the diffusion layer and reacts with the protons and electrons to form water and heat:

$$O_2+2H^++2e^- \rightarrow H_2O \quad (2)$$

Development of polymer membrane with high performance, thermal and water management is the subject that some studies have focused on. If the membrane has good thermal and protonic conductivity, it can remain hydrated and can conduct the protons better [10]. On the other hand, some investigations have focused on fuel cell structure design. These types of fuel cells have some advantages: low operating temperature (60-90^{o}C), simple design, low weight and volume and the prospect of further significant cost reduction make PEMFC technology a candidate for transport applications as well as for small appliances such as laptop computers.

Although there are more advantages in using fuel cell technology, but still, current PEMFCs are considerably more expensive compared with other power generation systems such as combustion engines and batteries. Therefore, it is critical to find a way to reduce cost and increase their power through engineering optimization. It requires a better understanding of PEMFCs and how various parameters affect their performance.

Experimental and theoretical studies on fuel cells have been conducted. Experimental studies of PEM fuel cells are prohibitive, so computer modeling is more cost effective and easier to do when design changes are made [11, 12].

In the past, to provide understanding about fuel cell performance, numerical and theoretical fuel cell modeling has been used extensively. Numerous researchers have focused on different aspects of the fuel cell:

Bernardi and Verbrugge [13, 14] investigated a one-dimensional, isothermal model which provides valuable information about the physics of the electrochemical reactions and transport phenomena in the gas diffusion, catalyst and membrane layer.

Fuller and Newman [15] published a quasi two-dimensional model of the MEA, which is based on concentration solution theory for the membrane and accounts for thermal effects.

Nguyen and White [16] proposed a two-dimensional and isothermal model. They considered water transport through membrane by the electro osmosis drag force as well as heat transfer from the solid phase to the gas phase along the flow channels.

Baschuk and Li [17] published a one-dimensional, steady-state model where they included the degree of water flooding in the gas-diffusion electrodes as a modeling parameter.

Gurau et al. [18] first used the methods of computational fluid dynamics for PEM Fuel Cell modeling. They developed a two dimensional, steady-state model of a whole fuel cell, i.e. both flow channels with the MEA in between. In their model, there was no interaction between gas and liquid phase of water.

The first three-dimensional modeling was done by Dutta et al. [19]. They obtained velocity, density and pressure contours in the gas diffusion layers. Their results showed that the current direction is drastically dependent on the mass transfer mechanism in the membrane electrode assembly.

Rezazadeh et al.[20] used an adaptive neuro-fuzzy inference system (ANFIS) for modeling proton exchange membrane fuel cell (PEMFC) performance using some numerically investigated data and compared them with those of experimental results for training and test data. Considering the results, their proposed model using ANFIS is efficient and valid and it can be expanded for more general states.

Pourmahmoud et al. [21] presented the results of a numerical investigation, using a comprehensive three-dimensional, single phase, non-isothermal and parallel flow model of a PEM fuel cell with deflected membrane electrode assembly (MEA).This numerical research has concentrated on the deflection parameter that affects the performance of this type of fuel cell.

This article presents the results of a numerical investigation using a comprehensive 3-dimensional, single phase, non-isothermal and parallel flow model of a PEM fuel cell with straight channels. The main objective of this work is to explain the mass transport phenomena, temperature variation and current density distribution of base model (model with straight flow channels). The model equations are then solved by a numerical method based on finite volume method (FVM). The model findings are then validated with the experimental data reported in Wang et al. [22] to verify its accuracy.

2. Model Equations and Assumptions

The proposed model is based on the following assumptions:

(1) The system operates under steady state condition.

(2) The flow regime in channels is supposed to be laminar for reactant gases because of low velocities gradient and eventually low Reynolds number.

(3) The incoming gas mixture behave as ideal gas.

(4) The gas diffusion layers, catalyst layers and membrane are isotropic and homogeneous porous

media; this asserts that the porosity is constant in the whole region of the gas diffusers.
(5) The membrane is considered impermeable for reactant gases.
(6) There is no interaction between the gas and liquid phase of water (the model is single phase).

3. Model Eequations

In this numerical simulation, a single domain model formation was used for the governing equations. These equations consist of:

A. Continuity equation

Electrodes are considered as a porous medium where reactant gases are distributed on catalyst layers. If ε is the porosity inside porous media:

$$\frac{\partial(\rho\varepsilon u)}{\partial x}+\frac{\partial(\rho\varepsilon v)}{\partial y}+\frac{\partial(\rho\varepsilon w)}{\partial z}=S_m \quad (3)$$

where S_m is mass source term, ρ mixture density, and u , v , and w are velocity components along x,y,z direction respectively. ε is the porosity; the fuel cell is a porous media. In the flow channels, this term is zero, because there is no reaction, but in the catalyst layers it is not zero due to reaction of reactant species:

$$S_{H2}=-\frac{M_{H2}}{2F}R_{an} \quad (4)$$

$$S_{O2}=-\frac{M_{O2}}{4F}R_{cat} \quad (5)$$

$$S_{H2O}=\frac{M_{H2O}}{2F}R_{cat} \quad (6)$$

S_{H2} and S_{O2} are negative, because they are being consumed, but S_{H2O} is positive due to its formation in catalyst layer. F is the Faraday constant and M the molecular weight of species. R_{an} and R_{cat} are the source terms which are calculated using the Butler-Volmer equation.

B. Momentum equation

In porous electrodes and for Newtonian fluid, the momentum equation can be written as:

$$\nabla.\left(\varepsilon\rho\vec{u}\vec{u}\right)=-\varepsilon\nabla p+\nabla.\left(\varepsilon\mu\nabla\vec{u}\right)+S_{mom} \quad (7)$$

where $\vec{u}$, p and μ are velocity vector, pressure, viscosity and momentum source term, respectively. The S_{mom} is used to describe Darcy's drag for flow through porous gas diffusion layers and catalyst layers as:

$$S_{mom}=-\frac{\mu}{\beta}\vec{u} \quad (8)$$

β is the gas permeability inside the porous media.

C. Mass transfer equation

The continuity equation in steady state conditions is written as follows:

$$\nabla.\left(\rho\varepsilon\vec{u}\,y_i\right)=-\nabla.\vec{J}_i+S_i \quad (9)$$

where y_i and $\vec{J}_i$ are mass fraction and diffusion mass flux vector, respectively. S_i is mass source term which has been presented in equations 4-6.
Fick's equation gives the diffusion mass flux vector:

$$\vec{J}_i=-\sum\rho D_{ij}^{eff}\nabla\vec{y}_i \quad (10)$$

Within porous electrodes, mass transfer equation changes to:

$$\nabla.\left(\rho\varepsilon\vec{u}\,y_i\right)=\nabla.\left(\rho\varepsilon D_{ij}^{eff}\nabla\vec{y}_i\right)+S_i \quad (11)$$

D_{ij}^{eff} is effective diffusivity of species estimated from the:

$$\varepsilon D_{ij}^{eff}=D_{ij}\times\varepsilon^{1.5} \quad (12)$$

D_{ij} is diffusivity of species inside .

D. Energy equation

The energy equation is given by:

$$\nabla.\left(\rho\varepsilon\vec{u}\vec{T}\right)=\nabla.\left(k_{eff}\nabla\vec{T}\right)+S_T \quad (13)$$

k_{eff} is the effective thermal conductivity which is calculated as volume average of solid and fluid conductivity in porous medium. S_T is source term and defined with the following equation:

$$S_T=I^2R_{ohm}+h_{reaction}+h_{phase} \quad (14)$$

Since phase change in numerical simulation was not considered, so h_{phase} would be omitted. $h_{reaction}$ is the heat generated through the chemical reactions and R_{ohm} is defined as:

$$R_{ohm}=\frac{t_m}{\sigma_{mem}} \quad (15)$$

where t_m and σ_{mem} are thickness and protonic conductivity of membrane, respectively.

$$\sigma_{mem}=\exp\left[1268\left(\frac{1}{303}-\frac{1}{T}\right)\right] \quad (16)$$
$$\left(0.005139\lambda-0.00326\right)$$

where water content in the membrane, λ , is defined as the number of water molecules per sulfonate group inside the membrane. The water content can be

expressed as a function of the water activity, a, by the following equation:

$$\lambda = 0.3 + 6a\left[1 - \tanh\left(a - 0.5\right)\right] + 3.9\sqrt{a}\left[1 + \tanh\left(\frac{a - 0.89}{0.23}\right)\right] \quad (17)$$

where the activity, a , is calculated by:

$$a = \frac{C_w RT}{P_{sat}} = \frac{P_w}{P_{sat}} \quad (18)$$

P_w , P_{sat} are water vapor and saturation pressure, respectively.

E. Charge conservation equation

As mentioned before, electrons transfer through conductive solid phase and protons transport through the membrane. So, two charge equations are needed:

$$\nabla.\left(\sigma_{sol}\nabla\varnothing_{sol}\right) + R_{sol} = 0 \quad (19)$$

$$\nabla.\left(\sigma_{mem}\nabla\varnothing_{mem}\right) + R_{mem} = 0 \quad (20)$$

σ_{sol} and σ_{mem} are electrical conductivity of electrodes and membrane (S/m), respectively. $\varnothing_{sol}$ and $\varnothing_{mem}$ are defined as potential of electron and proton, respectively. R_{sol} and R_{mem} are source terms (they are current density (A/m^3)). These terms are only defined in the catalyst layers:

For the solid phase:

$R_{sol} = -R_{an}(<0)$ Anode side

$R_{sol} = R_{cat}(>0)$ Cathode side

For the membrane phase:

$R_{mem} = R_{an}(>0)$ Anode side

$R_{mem} = -R_{cat}(<0)$ Cathode side

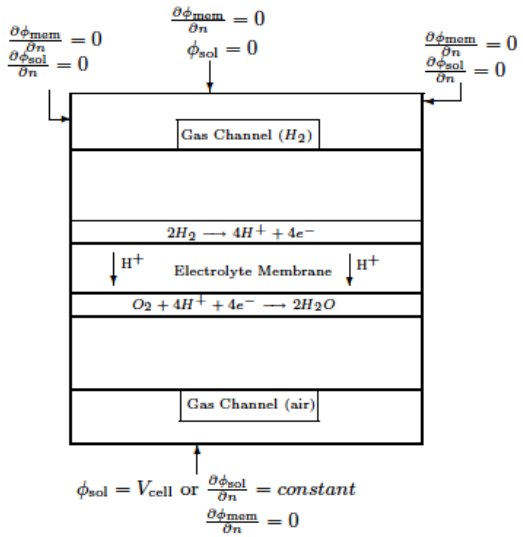

Fig. 1. Boundary conditions

The source terms are calculated using the Butler-Volmer equation:

$$R_{an} = J_{an}^{ref}\left(\frac{[H_2]}{[H_2]_{ref}}\right)^{\gamma_{an}}\left(e^{\left(\alpha_{an}F/RT\right)\eta_{an}} - e^{-\left(\alpha_{cat}F/RT\right)\eta_{cat}}\right) \quad (21)$$

$$R_{cat} = J_{cat}^{ref}\left(\frac{[O_2]}{[O_2]_{ref}}\right)^{\gamma_{cat}}\left(e^{-\left(\alpha_{cat}F/RT\right)\eta_{cat}} - e^{\left(\alpha_{an}F/RT\right)\eta_{an}}\right) \quad (22)$$

J^{ref} is reference exchange current density (A/m^2).

4. Water transport through membrane

Water molecules in PEM fuel cell are transported via electro-osmotic drag due to the properties of polymer electrolyte membrane in addition to the molecular diffusion. H^+ protons transport water molecules through the polymer electrolyte membrane and this transport phenomenon is called electro-osmotic drag. In addition to the molecular diffusion and electro-osmotic drag, water is also produced in the catalyst layers due to the electrochemical reaction.

The assumption of single phase model is used here. It means that water generated from the cathodic equation is in a vapor state.

5. Boundary conditions

Constant mass flow rate at the channel inlet and constant pressure are the conditions at the channel outlet, and the no-flux conditions are executed for mass, momentum, species and potential conservation equations at all boundaries expect for inlets and outlets of the anode and cathode flow channels. Fig.1 shows the other surface boundary conditions.

6. Numerical implementation

For solving the equations, the SIMPLE algorithm is applied. In addition, the main procedure for solving the governing equations with the appropriate boundary conditions is finite volume method and implicit solver. Figure 2 shows the algorithm for numerical simulation of model equations.

In the base model, the structured meshes are used and in catalyst layers where the electro chemical reactions occur, the meshes are finer. Also, grid-independence test was implemented, and finally the optimum number of meshes (174 000) chosen. Fig. 3 indicates the computational domain of base model (its components are listed in Figure 1.

A series of simulation were carried out on the model from low to high operating current densities. In order to evaluate the validity of the model, numerical simulation results (for conventional model) were compared with the experimental data presented by Wang et al. [22], as shown in Figure 4, which shows

a favorable agreement between them.

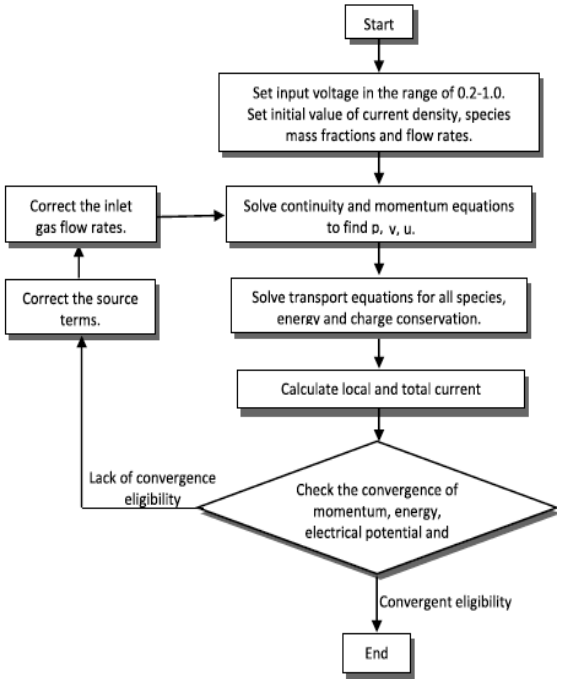

Fig. 2. Numerical implementation

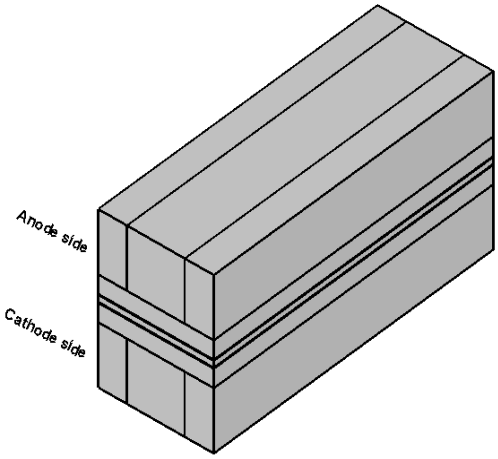

Fig. 3. Computational domain of numerical model

As it is clear from Figure 4, there is a non-concurrence between the numerical simulation results and experimental data especially at the high current density region. This fact is the result of the single phase assumption. In other words, the water produced in the catalyst layer is in the vapor phase (in numerical simulation). In fact, liquid water fills the pores of the catalyst and gas diffusion layers and do not let the oxygen molecules transfer to the catalyst layer easily. So, the mass transfer resistance of reactants (concentration loss) increases at the high current density region. The power density curve for the model is illustrated too. There is a relation between voltage, current density and the power of the fuel cell as P =V.I.

Fuel cell operating condition and geometric parameters are shown in Table 1.

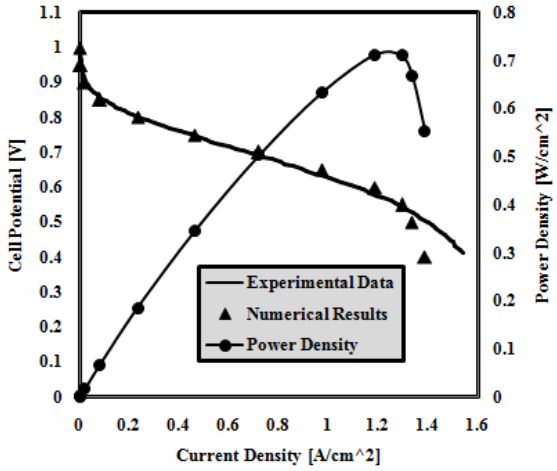

Fig. 4. Numerical results and experimental data comparison

Table 1. Geometrical parameters and operating conditions

Parameter	value
Anode & Cathode pressure	3 atm
Anode & Cathode humidity	100%
Gas channel length	7.0×10^{-2} m
Gas channel width and depth	1.0×10^{-3} m
Bipolar plate width	5.0×10^{-4} m
Gas diffusion layer thickness	3.0×10^{-4} m
Catalyst layer thickness	1.29×10^{-5} m
Cell temperature	70°C
Porosity	4
Stoichiometry	2

The first important parameter which should be explained is temperature distribution, especially along the cell width. The temperature affects various factors of the fuel cell. As it is clear from Figures 5, 6, and 7 the temperature at the regions next to the bipolar plates is lower; because bipolar plates are good thermal conductors and cause the better heat transfer; this fact leads to temperature reduction at the shoulder regions. The slight temperature decrease along the flow direction is probably because of water level and its distribution. The electrochemical reaction occurring in the cathode catalyst layer has two significant

roles: water formation and temperature rise (so the cathode side temperature is higher than that of the anode side). In this model, the higher temperature distribution is at 0.4V and this is due to high reaction rate in the fuel cell. High current densities (or low voltages) cause the reactants to react faster and subsequently the temperature rises. The high rate of water production along the cell assists cooling of the cell especially at exit region of the cell; therefore, high temperature losses will happen in this voltage.

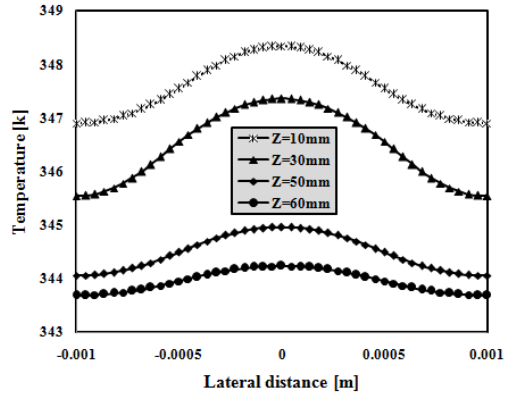

V=0.4[V]

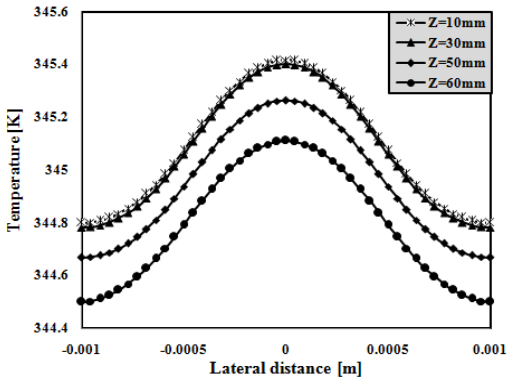

V=0.6[V]

Fig. 5. Temperature at cathode catalyst layer and membrane interface

Figure 8 indicates that water is building up along the flow direction. This is the result of two important phenomena: water formation at the cathode catalyst layer, and water transferring due to electro-osmotic drag from anode to cathode side. More water present at the exit region of fuel cell cools the cell and reduces the temperature. It is found that the water molecules at the inlet of the anode channel are transported mostly to the cathode by electro-osmotic drag, but the electro-osmotic mass flux decreased along the channel.

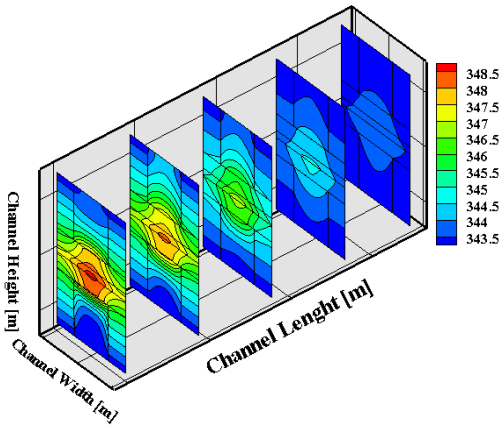

Fig. 6. Temperature distribution contour at different cross sections at V=0.4[V]

As shown in the Figure 9, the amount of back diffusion was much smaller than the electro-osmotic mass flux. Therefore, the net water mass transfer across the membrane is directed from anode to cathode side.

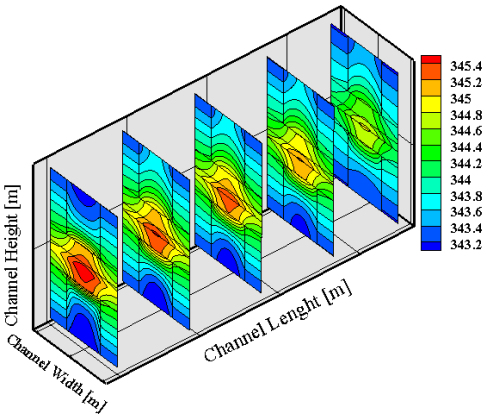

Fig. 7. Temperature distribution contour at different cross sections at V=0.6[V]

Equation 18 states that the anode water activity is inversely related to temperature. Since the temperature is decreasing along the flow direction, consequently the anode water activity is increasing Figure10. In addition, the water in the anode catalyst layer is responsible for transporting the hydrogen protons to the cathode side, so its value should be reduced along the flow direction from inlet to outlet Figure 11 and since the amount of oxygen in the longitudinal direction reduces (its consumption increases) and the amount of water increases, more H^+ should be transported by water molecules. The lower the cell voltages, the more water molecules transfer from anode to cathode

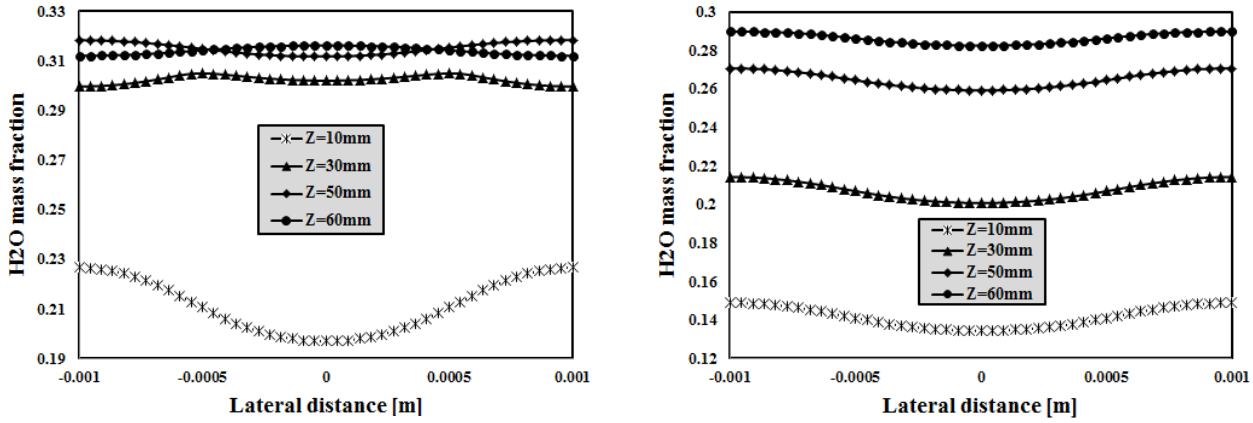

V=0.4[V] V=0.6[V]

Fig. 8. Water mass fraction at cathode catalyst layer and membrane interface

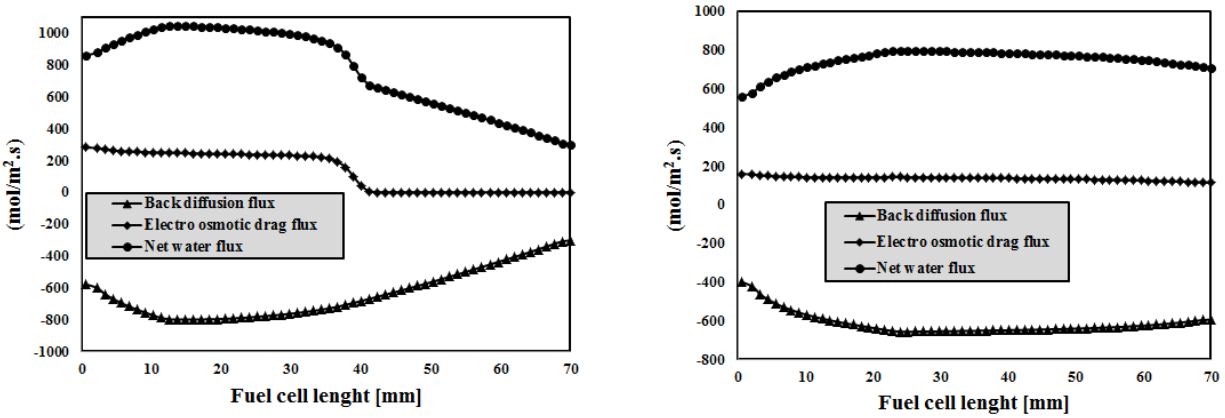

V=0.4[V] V=0.6[V]

Fig. 9. Water flux along the fuel cell

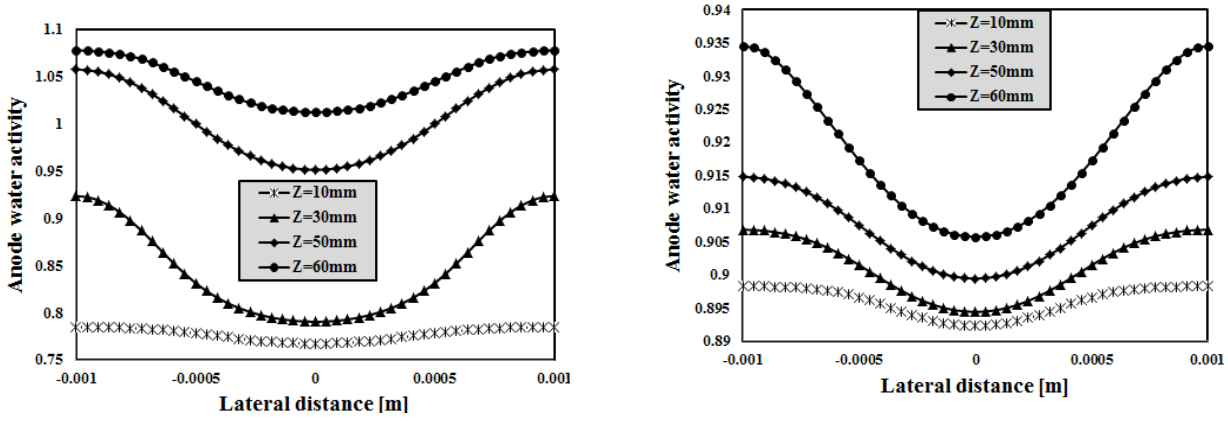

V=0.4[V] V=0.6[V]

Fig.10. Anode water activity at anode catalyst layer and membrane interface

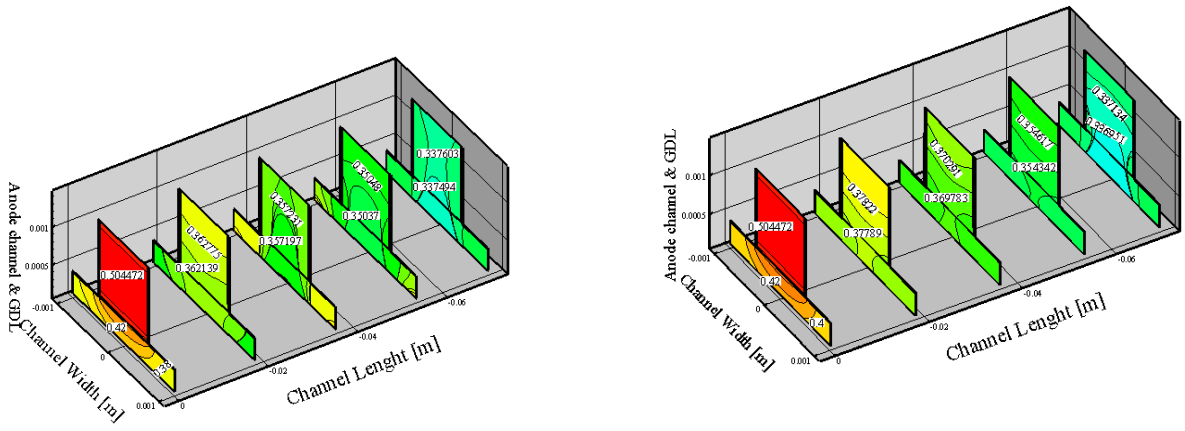

V=0.4[V] V=0.6[V]

Fig.11. Anode side water distribution at different planes of channel and GDL

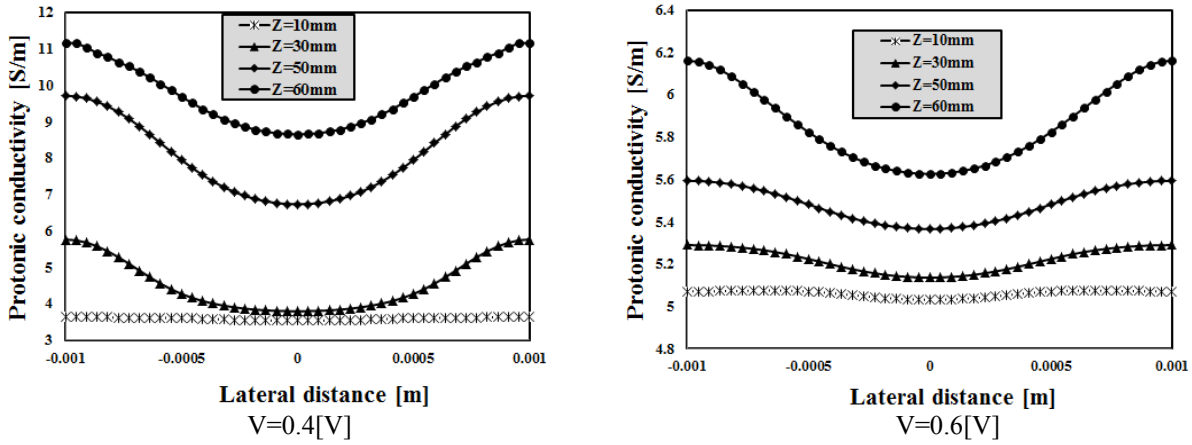

V=0.4[V] V=0.6[V]

Fig. 12. Protonic conductivity at anode catalyst layer and membrane interface

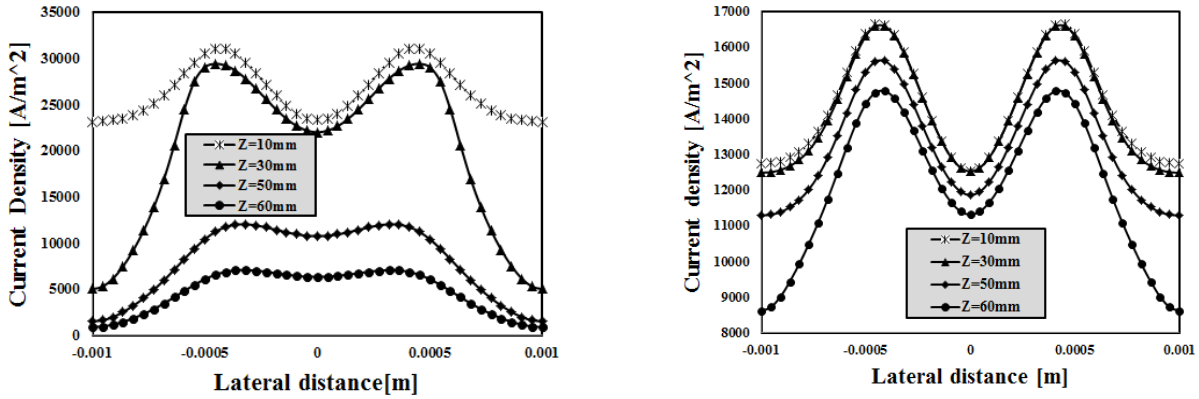

V=0.4[V] V=0.6[V]

Fig. 13. Current density magnitude at cathode catalyst later and membrane interface

The governing parameters of fuel cell are highly dependent on each other. One of these important parameters is membrane protonic conductivity. This factor is strongly dependent on temperature (inversely) and anode water activity (directly), hence

its magnitude at the shoulder region is higher than at the channel region (Figure12).

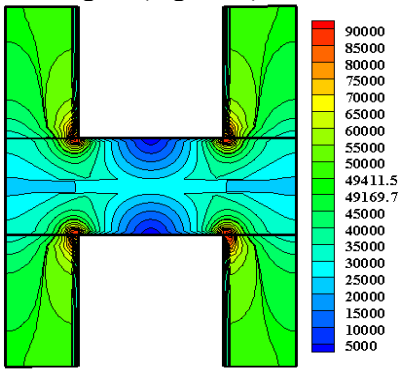

V=0.4[V] at Z=0mm

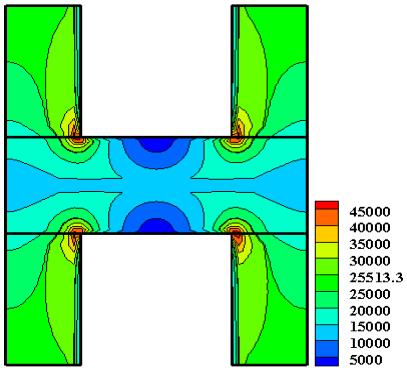

V=0.6[V] at Z=0mm

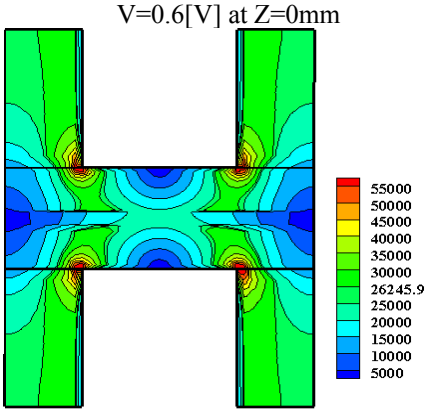

V=0.4[V] at Z=36mm

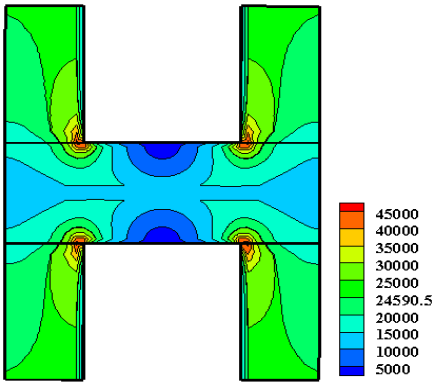

V=0.6[V] at Z=36mm

Fig. 14. Current density distribution at different cross sections

According to equation 23, ohmic loss is directly related to membrane thickness (t_m) and current density (I). It is also inversely related to membrane protonic conductivity (σ_m).

$$R_{ohm} = \frac{t_m}{\sigma_e} \rightarrow \eta_{ohm} = IR_{ohm} \quad (23)$$

Figures 13 and 14 illustrate the current density distribution at the interface of cathode catalyst and membrane. Current density indeed is electron flux in the cell and while electrons flow through the solid phase (solid phase of gas diffusion and catalyst layers), they want to traverse the shortest path to achieve the bipolar plates, therefore, its value is higher at the shoulder region. In addition, current density amount dwindles along the flow direction. As it has been mentioned before, the water building up along the cathode catalyst layer (especially at low voltages or high current densities) blocks the pores of the porous media and consequently prevents the oxygen reaching the reaction area. This fact leads to current density reduction along the flow direction.

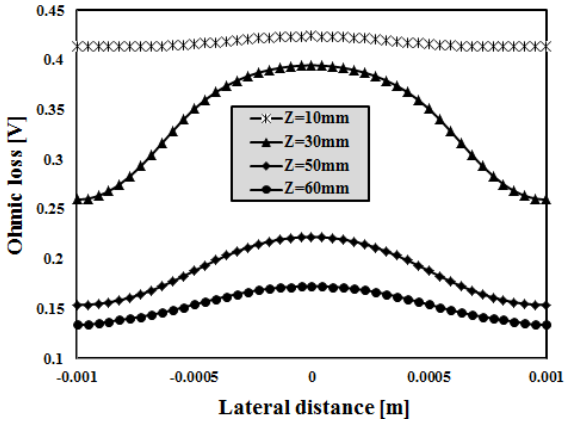

V=0.4[V]

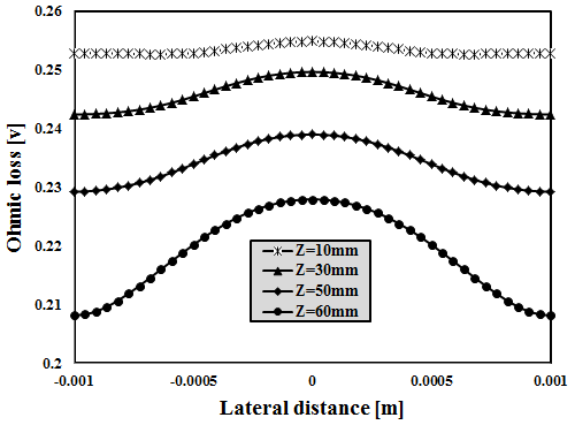

V=0.6[V]

Fig. 15. Ohmic loss at cathode catalyst later and membrane interface

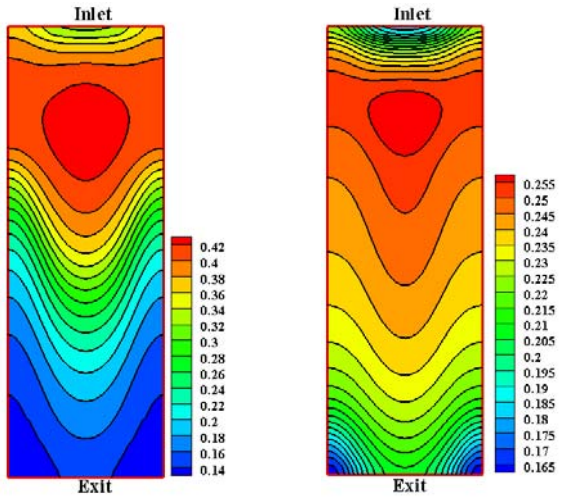

V=0.4[V] V=0.6[V]

Fig. 16. Ohmic loss contour at cathode catalyst layer and membrane interface

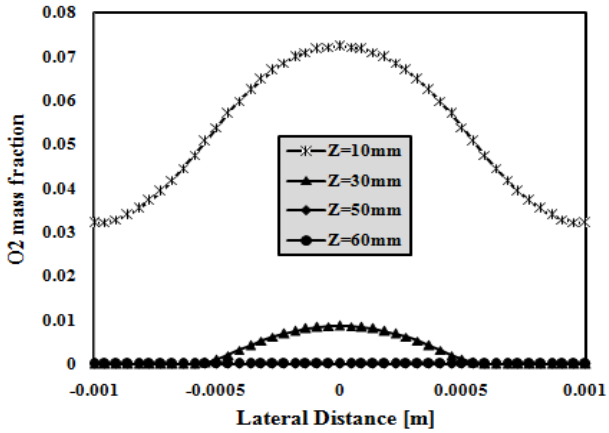

V=0.4[V]

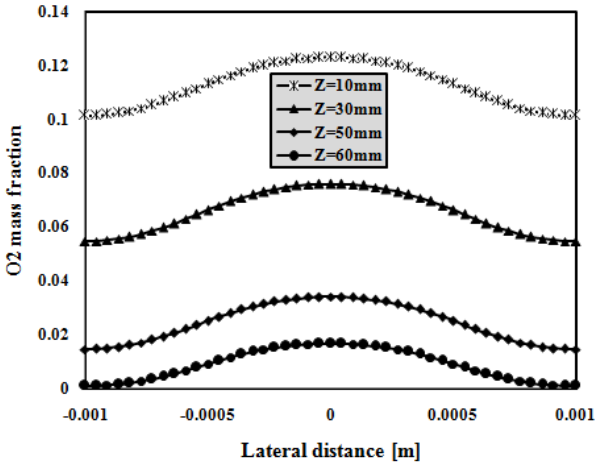

V=0.6[V]

Fig. 17. Oxygen mass fraction at cathode catalyst layer and membrane interface

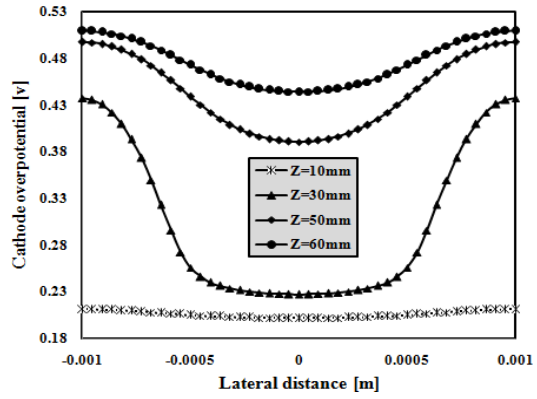

V=0.4[V]

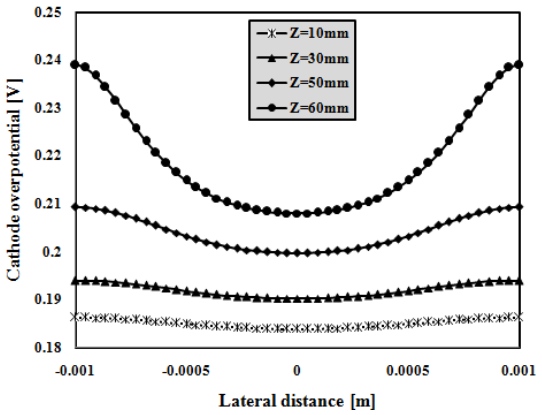

V=0.6[V]

Fig. 18: Cathode over potential at cathode catalyst layer and membrane interface

One of parameters affected by the oxygen distribution is cathode over-potential. Wherever the fuel cell faces lack of oxygen (the reason was discussed before and illustrated in Figure 17, the cathode over-potential is high (as illustrated in Figure 18).

Oxygen and water mass fraction distributions along the cathode catalyst and membrane interface are presented in Figures 19-22. As mentioned before, the quantity of oxygen decreases (due to its consumption) and that of water increases (due to its formation).

The reduction of oxygen during the cell operation at different voltages has been investigated. This comparison has been done along the cell at cathode catalyst layer and membrane interface. As we can see in the paper, that oxygen mass fraction is reduced along the cell. In the catalyst layer, oxygen level can be balanced by the its consumption, and also injection of oxygen to the catalyst layer because of oxygen concentration gradient. The low diffusion of oxygen along the fuel cell which is due to low concentration

of oxygen in the inlet air leads to significant lack of oxygen in the cell. In the high operating voltage which produces low current density, oxygen consumption rate is low enough, so that it does not cause diffusion problems. But, in low voltages the oxygen concentration rates sometimes reaches zero. Problems related to diffusion of hydrogen on the anode and oxygen at the cathode are similar.

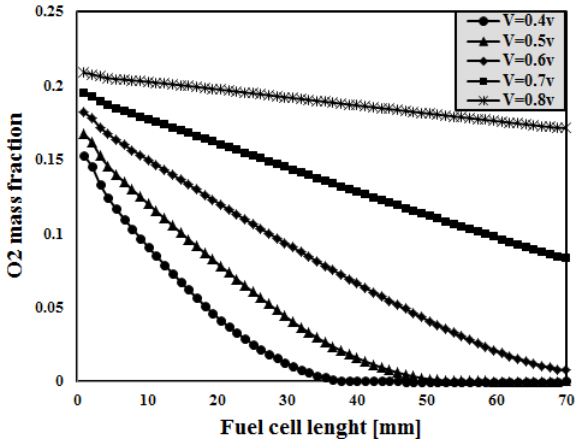

Fig. 19. Oxygen mass fraction along the cell at cathode catalyst layer and membrane interface

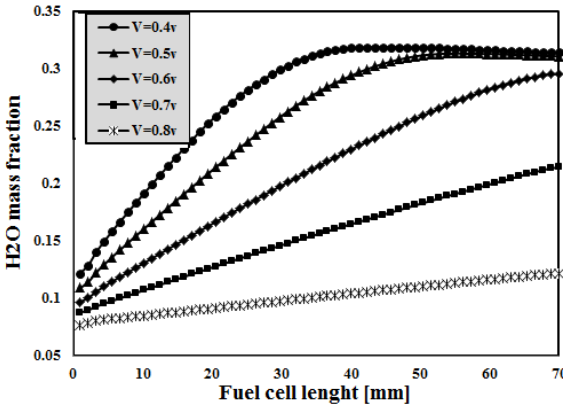

Fig. 20. Water mass fraction along the cell at cathode catalyst layer and membrane interface

It is clear that for V=0.4, 0.5 [V], oxygen gradually approaches zero and water reaches to its maximum value and remains constant; because at these voltages, extra water blocks the pores of the gas diffusion layer and hampers the oxygen penetration to the cathode catalyst layer (concentration loss). The extra water produced has an important role in cooling fuel cell (temperature reduction), as shown in Fig.23. As it can be concluded from results, there is a logical relation between all of the operating parameters of fuel cell.

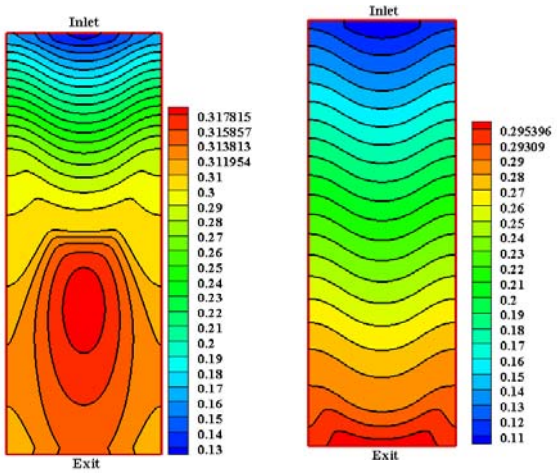

V=0.4[V] V=0.6[V]

Fig. 21. Water mass fraction contour along the cell at cathode catalyst layer and membrane interface

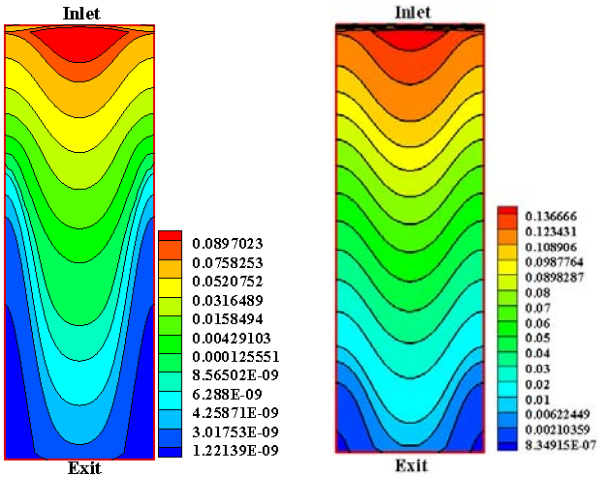

V=0.4[V] V=0.6[V]

Fig. 22. Oxygen mass fraction contour along the cell at cathode catalyst layer and membrane interface

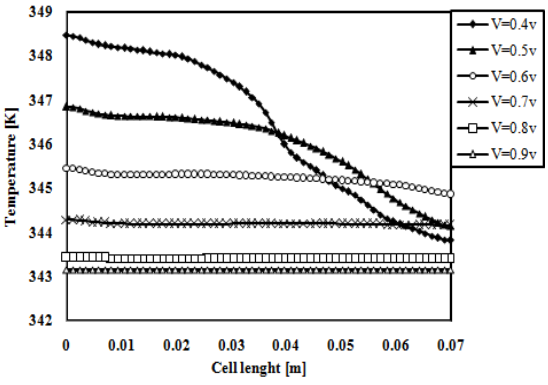

Fig. 23. Temperature distribution along the cell for different cell voltages at cathode catalyst layer and membrane interface

7. Conclusions

In this article a three dimensional computational fluid dynamics model of a Proton Exchange Membrane Fuel Cell (PEMFC) with straight flow channels has been simulated. In the present research, some parameters such as oxygen consumption, water production, temperature distribution, ohmic losses, anode water activity, cathode over-potential and the fuel cell performance for straight single cell have been investigated in more detail.

Temperature affects various factors of the fuel cell. The temperature at the regions adjacent to the bipolar plates is lower. Since bipolar plates are good thermal conductors and cause better heat transfer, bipolar geometrical designing with better materials can be important problems to study. In addition, electrons flow through the bipolar to the external circuit to produce electrical power. So, the current density is higher at the shoulder regions; this fact affects the species and other important parameters distribution inside the cell.

On the other hand, the numerical simulations reveal that these important operating parameters are highly dependent to each other and the fuel cell efficiency is affected by the kind of species distribution. So, for especial uses in desirable voltages, these numerical results can be useful for preventing from the unwilling losses..

Finally, the numerical results for base model showed good agreement with the experimental data.

8. Nomenclature

A_{MEA}	Surface area of electrode-membrane assembly (m^2)
A_{ch}	Channel cross section (m^2)
B	Electrode diffusivity (m^2)
CH_2	Local concentration of hydrogen (mol m^{-3})
CO_2	Local concentration of oxygen (mol m^{-3})
E	Porosity
F	Faraday constant (C mol^{-1})
H	Surface over potential (V)
k	Electrical conductivity of bipolar plate(S m^{-1})
k_{eff}	Thermal conductivity of electrode ($Wm^{-1}K^{-1}$)
M	Dynamic viscosity (kg s m^{-2})
M	Molecular weight (g mol^{-1})
M_m	Dry membrane weight (kg)
P	Density (kg m^{-3})
R_{an}	Exchange current density of anode (A m^{-3})
R_{cat}	Exchange current density of cathode(A m^{-3})
S	Sink source
U	Velocity in x direction (m s^{-1})
V	Velocity in y direction (m s^{-1})
W	Velocity in z direction (m s^{-1})

Greek symbols

σ_{mem}	Electrical conductivity of membrane(S m^{-1})
σ_{sol}	Electrical conductivity of electrode (S m^{-1})
α_{an}	Anode charge transport coefficient
α_{cat}	Cathode charge transport coefficient
Λ	Water content of membrane

9. References

1. Arasti M.R., Bagheri Moghaddam N. Use of technology mapping in identification of fuel cell sub-technologies. Int J Hydrogen Energ, 2010, 35, 9516–9525.
2. Sadeghzadeh K., Salehi M.B. Mathematical analysis of fuel cell strategic technologies development solutions in the automotive industry by the TOPSIS multi-criteria decision making method. Int J Hydrogen Energ, 2011, 36, 13272–13280.
3. Zaidi S.M.J., Rahman S.U., Zaidi H.H. R&D activities of fuel cell research at *KFUPM, Desalination.* 2007, 209, 319–327.
4. Ashraf Khorasani M.R., Asghari S., Mokmeli A., Shahsamandi M.H., Faghih Imani B. A diagnosis method for identification of the defected cell(s) in the PEM fuel cells. Int J Hydrogen Energ, 2010, 35, 9269–9275.
5. Costamagna P., Srinivasan S. Quantum jumps in the PEMFC science and technology from the 1960s to the year 2000: part I. Fundamental scientific aspects. J Power Sources, 2001, 102, 242–252.
6. Rismanchi B., Akbari M.H. Performance prediction of proton exchange membrane fuel cells using a three-dimensional model. Int J Hydrogen Energ, 2008, 33, 439–448.
7. Akbari M.H., Rismanchi B. Numerical investigation of flow field configuration and contact resistance for PEM fuel cell performance. Renewable Energ, 2008, 33, 1775–1783.
8. Khajeh-Hosseini-Dalasm N., Kermani M.J., Moghaddam D.G., Stockie J.M. A parametric study of cathode catalyst layer structural parameters on the performance of a PEM fuel cell. Int J Hydrogen Energ, 2010, 35, 2417–2427.
9. Mokmeli A., Asghari S. An investigation into the effect of anode purging on the fuel cell performance. Int J Hydrogen Energ, 2010, 35, 9276–9282.
10. Jang J.-H., Yan W.-M., Shih C.-C. Numerical study of reactant gas transport phenomena and cell performance of proton exchange membrane fuel cells. J Power Sources, 2006, 156, 244–252.
11. Hontañón E., Escudero M.J., Bautista C., García-Ybarra P.L., Daza L. Optimisation of flow-field in polymer electrolyte membrane fuel

cells using computational fluid dynamics techniques. J Power Sources, 2000, 86, 363–368.
12. Yan W.-M., Li H.-Y., Chiu P.-C., Wang X.-D. Effects of serpentine flow field with outlet channel contraction on cell performance of proton exchange membrane fuel cells. J Power Sources, 2008, 178, 174–180.
13. Bernardi D.M., Verbrugge M.W. Mathematical Model of a Gas Dissusion Electrode Bonded to a Polymer Electrolyte. AIChE J, 1991, 37(8):1151–1163.
14. Bernardi D.M., Verbrugge M.W. A Mathematical Model of the Solid- Polymer-Electrolyte Fuel Cell. J Electrochem Soc, 1992, 139(9):2477–2491.
15. Fuller T. F., Newman J. Water and Thermal Managament in Solid-Polymer-Electrolyte Fuel Cells. J Electrochem Soc, 1993, 140(5):1218–1225.
16. Nguyen T.V., White R.E. Water and heat management model for proton-exchange-embrane fuel cells. J Electrochem Soc, 1993, 140, 2178–2186.
17. Baschuk J.J., Li X. Modelling of polymer electrolyte membrane fuel cells with variable degrees of water ‡ooding. J Power Sources, 2000, 86:181–195.
18. Gurau V., Liu H., Kakac S. “Two-Dimensional Model for Proton Exchange Membrane Fuel Cells”. AIChE J. 1998, 44(11):2410–2422.
19. Dutta S., Shimpalee S., Van Zee J.W. Numerical prediction of mass-exchange between cathode and anode channels in a PEM fuel cell. Int J Heat Mass Transfer, 2001, 44, 2029–2042.
20. Rezazadeh S., Mehrabi M., Pashaee T., Mirzaee I. Using adaptive neuro-fuzzy nference system (ANFIS) for proton exchange membrane fuel cell (PEMFC) performance modeling. J Mechanical Sci Technol, 2012, 26(11), 3701~3709.
21. Pourmahmoud N., Rezazadeh S., Mirzaee1 I, Motaleb F.S. A computational study of a three-dimensional proton exchange membrane fuel cell (PEMFC) with conventional and deflected membrane electrode assembly. J Mechanical Sci Technol, 26 (9) (2012) 2959~2968.
22. Wang L., Husar A., Zhou T., Liu H. Int J Hydrogen Energ, 2003, 28(11), 1263-1272.